

# Towards Latent Space Optimality for Auto-Encoder Based Generative Models

Arnab Kumar Mondal\*  
IIT Delhi  
anz188380@cse.iitd.ac.in

Sankalan Pal Chowdhury\*  
IIT Delhi  
cs1160701@iitd.ac.in

Aravind Jayendran\*  
Flipkart Internet Pvt. Ltd.†  
aravind.j@flipkart.com

Parag Singla  
IIT Delhi  
parags@cse.iitd.ac.in

Himanshu Asnani  
TIFR  
himanshu.asnani@tifr.res.in

Prathosh AP  
IIT Delhi  
prathoshap@ee.iitd.ac.in

## Abstract

*The field of neural generative models is dominated by the highly successful Generative Adversarial Networks (GANs) despite their challenges, such as training instability and mode collapse. Auto-Encoders (AE) with regularized latent space provides an alternative framework for generative models, albeit their performance levels have not reached that of GANs. In this work, we identify one of the causes for the under-performance of AE-based models and propose a remedial measure. Specifically, we hypothesise that the dimensionality of the AE model’s latent space has a critical effect on the quality of the generated data. Under the assumption that nature generates data by sampling from a “true” generative latent space followed by a deterministic non-linearity, we show that the optimal performance is obtained when the dimensionality of the latent space of the AE-model matches with that of the “true” generative latent space. Further, we propose an algorithm called the Latent Masked Generative Auto-Encoder (LMGAE), in which the dimensionality of the model’s latent space is brought closer to that of the “true” generative latent space, via a novel procedure to mask the spurious latent dimensions. We demonstrate through experiments on synthetic and several real-world datasets that the proposed formulation yields generation quality that is better than the state-of-the-art AE-based generative models and is comparable to that of GANs.*

## 1. Introduction

The primary objective of a generative model is to sample from the data generating distribution. Deep generative models, especially the Generative Adversarial Networks (GANs) [11] have shown remarkable success in this task by generating high quality data [6]. GANs implicitly learn to

sample from the data distribution by transforming a sample from a simplistic distribution (such as Gaussian) to the sample from the data distribution by optimising a min-max objective through an adversarial game between a pair of function approximators called the generator and the discriminator. Although GANs generate high-quality data, they are known to suffer from problems like instability of training [4, 32], degenerative supports for the generated data (mode collapse) [2, 33] and sensitivity to hyper-parameters [6].

Auto-Encoder (AE) based generative models provide an alternative to GAN based models [39, 20, 28, 35]. The fundamental idea is to learn a lower dimensional latent representation of data through a deterministic or stochastic encoder and learn to generate (decode) the data through a decoder. Typically, both the encoder and decoder are realised through learnable family of function approximators or deep neural networks. To facilitate the generation process, the distribution of the latent space is forced to follow a known distribution so that sampling from it is feasible. Despite resulting in higher data-likelihood and stable training, the quality of generated data of the AE-based models is known to be far away from state-of-the-art GAN models [10, 12, 34].

While there have been several angles of looking at the shortcomings of the AE-based models [10, 17, 19, 36, 21, 5, 37], an important question seems to have remained unaddressed - *What is the “optimal” dimensionality of the latent space  $\mathcal{Z}$  to ensure good generation in AE-based models?* It is a well-known fact that most of the naturally occurring data effectively lies in a manifold with dimension much lesser than its original dimensionality [8, 24, 29]. Intuitively, this suggests that with *well-behaved* functions (such as Deep Neural Networks) it is difficult to optimally represent such data using latent dimensions less or more than the effective manifold dimensionality. Specifically, “lesser” number of dimensions in  $\mathcal{Z}$  may result in loss of information and “extra” dimensions may lead to noise in gener-

\*these authors contributed equally

†work done when at IIT Delhi

ated data when this latent space is used as input to a generative neural network. This observation is also corroborated with empirical evidence provided in Fig. 3 where an AE-based generative model is constructed on synthetic and MNIST [25] datasets, with varying latent dimensionality (everything else kept the same) and shown that the standard generation quality metric follows a peaky U-shaped curve. Motivated by the aforementioned observations, we explore the role of latent dimensionality on the generation quality of AE-models with following contributions:

1. We provide theoretical understanding on the role of the dimensionality of the latent space on the quality of AE-based generative models.
2. We model the data generation as a two-stage process comprising of sampling from a “true” latent space followed by a deterministic function and show that under this model, the optimal generation quality is achieved by an AE-model when the latent dimensionality of the AE-model is exactly equal to that of the “true” latent space that is assumed to generate data.
3. Owing to the obliviousness of the dimensionality of the “true” latent space in real-life data, we propose a method to algorithmically “mask” the spurious dimensions in AE-based models.
4. We demonstrate the efficacy of the proposed model on synthetic as well as large-scale image datasets by achieving better generation quality metrics compared to the state-of-the-art (SOTA) AE-based models. We also show that the proposed method ensures that the effective active dimensions remain the same irrespective of the initially assumed latent dimensionality.

## 2. Related work

Let  $\mathbf{x}$  denote data points lying in the space  $\mathcal{X}$  conforming to an underlying distribution  $\Upsilon(\mathbf{x})$ , from which a generative model desires to sample. An Auto-Encoder based model constructs a lower-dimensional latent space  $\mathcal{Z}$  (conforming to a distribution  $\Pi(\mathbf{z})$ ) to which the data is projected through an (probabilistic or deterministic) Encoder function,  $E_{\kappa}$ . An inverse projection map is learned from the  $\mathcal{Z}$  to  $\mathcal{X}$  through a Decoder function  $D_{\psi}$ , which can be subsequently used as a sampler for  $\Upsilon(\mathbf{x})$ . For this to happen, it is necessary that the latent space  $\mathcal{Z}$  is regularized to facilitate explicit sampling from  $\Pi(\mathbf{z})$ , so that decoder can generate data taking samples from  $\Pi(\mathbf{z})$  as input. Most of the AE-based models take the route of maximizing a lower bound constricted on the data likelihood which is shown [20, 16] to consist of the sum of two primary terms - (i) the likelihood of the data generated by the Decoder network - and (ii)

the divergence measure between the the assumed latent distribution,  $\Pi(\mathbf{z})$ , and the distribution imposed on the latent space by the Encoder,  $\Psi(\mathbf{z}) = \int \Psi(\mathbf{z}|\mathbf{x})\Upsilon(\mathbf{x})d\mathbf{x}$ , [16, 28]. This underlying commonality, suggests that the success of an AE-based generative model depends upon simultaneously increasing the likelihood of the generated data and reducing the divergence between  $\Psi(\mathbf{z})$  and  $\Pi(\mathbf{z})$ . The former of the criteria is fairly easily ensured in all AE models by minimizing a surrogate function such as the reconstruction error between the samples of the true data and output of the decoder. It is observed that, with enough capacity, this can be made arbitrarily small [7, 10, 1]. It is well recognized that the quality of the generated data relies heavily on achieving the second criteria of bringing the Encoder imposed latent distribution  $\Psi(\mathbf{z})$  close to the assumed latent prior distribution  $\Pi(\mathbf{z})$  [10, 16, 7]. This can be achieved either by (i) assuming a pre-defined primitive distribution for  $\Pi(\mathbf{z})$  and modifying the Encoder such that  $\Psi(\mathbf{z})$  follow assumed  $\Pi(\mathbf{z})$  [20, 28, 35, 9, 15, 18, 19] or by (ii) modifying the latent prior  $\Pi(\mathbf{z})$  to follow whatever distribution ( $\Psi(\mathbf{z})$ ) Encoder imposes on the latent space [36, 5, 21, 17, 37].

The seminal paper on VAE [20] proposes a probabilistic Encoder which is tuned to output the parameters of the conditional posterior  $\Psi(\mathbf{z}|\mathbf{x})$  which is forced to follow the Normal distribution prior assumed on  $\Pi(\mathbf{z})$ . However, the minimization of the divergence between the conditional latent distribution and the prior in the VAE leads to trade-off between the reconstruction quality and the latent matching, as this procedure also leads to the minimization of the mutual information between  $\mathcal{X}$  and  $\mathcal{Z}$  which in turn reduces Decoder’s ability to render good reconstructions [18]. This issue is partially mitigated by altering the weights on the two terms of the ELBO during optimization [15, 7], or through introducing explicit penalty terms in the ELBO to strongly penalize the deviation of  $\Psi(\mathbf{z})$  from assumed prior  $\Pi(\mathbf{z})$  [9, 18]. Adversarial Auto-Encoders (AAE) [28] and Wasserstein Auto-Encoders (WAE) [35] address this issue, by respectively using adversarial learning and maximum mean discrepancy to match  $\Psi(\mathbf{z})$  and  $\Pi(\mathbf{z})$ . There also have been attempts in employing the idea of normalizing flow for distributional estimation for making  $\Psi(\mathbf{z})$  close to  $\Pi(\mathbf{z})$  [19, 30]. These methods although improving the generation quality over vanilla VAE while providing additional properties such as disentanglement in the learned space, fail to reach GAN-level generation quality.

In another class of methods, the latent prior  $\Pi(\mathbf{z})$  is made learnable instead of being fixed to a primitive distribution so that it matches with Encoder imposed  $\Psi(\mathbf{z})$ . In VamPrior [36], the prior is taken as a mixture density whose components are learned using pseudo-inputs to the Encoder. [21] introduces a graph-based interpolation method to learn the prior in a hierarchical way. Two-stage-VAE constructs two VAEs, one on the dataspace and the second on the latent

space of the first stage VAE [10]. [37, 23] employ discrete latent space using vector quantization schemes and fits the prior using a discrete auto-regressive model.

While all these models have proposed pragmatic methods on matching the distributions through changing the distributional forms, a couple of important related questions seem to be unaddressed - (a) What is the best that one can achieve despite a simplistic unimodal prior such as Gaussian and (ii) What is the effect of the latent dimensionality on generation quality in such case? Here, we focus on addressing these.

### 3. Effect of Latent Dimensionality

#### 3.1. Preliminaries

In this section, we theoretically examine the effect of latent dimensionality on quality of generated data in AE. We show that it's impossible to simultaneously achieve both R1 and R2 unless  $\mathcal{Z}$  has a certain *optimal* dimensionality. Specifically, we show that if dimensionality of  $\mathcal{Z}$  is more than the *optimal* dimensionality,  $\Pi(z)$  and  $\Psi(z)$  diverge too much (Lemma 2 and 3) whereas it being less leads to information loss (Lemma 1).

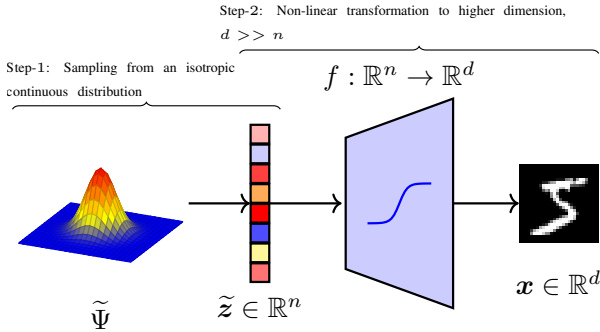


Figure 1. Depiction of assumed data generation process.

We allow a certain inductive bias in assuming that nature generates the data as in Figure 1 using the following two step process: First sample from some isotropic continuous latent distribution in  $n$ -dimensions (call this  $\Psi$  over  $\tilde{\mathcal{Z}}$ ), and then pass this through a function  $f : \mathbb{R}^n \rightarrow \mathbb{R}^d$ , where  $d$  is the dataset dimensionality. Typically  $d \gg n$ , thereby making data to lie on a low-dimensional manifold in  $\mathbb{R}^d$ . Since  $\tilde{\mathcal{Z}}$  can intuitively be viewed as the latent space from which the nature is generating the data, we call  $n$  as the *true latent dimension* and function  $f$ , as the *data-generating function*. Note that within this ambit,  $\tilde{\mathcal{Z}}$  forms the domain for  $f$ . We further cast the following benign assumptions on the function  $f$ :

A1  $f$  is *injective*: This assumption follows from the uniqueness of the underlying true latent variable  $\tilde{z}$ , given a data point.

A2  $f$  is *L-lipschitz*:  $\exists$  some finite  $L \in \mathbb{R}^+$  satisfying  $\|f(\tilde{z}_1) - f(\tilde{z}_2)\| \leq L\|\tilde{z}_1 - \tilde{z}_2\|$ ,  $\forall \tilde{z}_1, \tilde{z}_2 \in \tilde{\mathcal{Z}}$ .

A3  $f$  is *differentiable* almost everywhere.

Since universal function approximators such as Deep neural networks are shown to successfully generate data from that adhere to assumptions made above on  $f$ , it is reasonable to impose them on data-generating function. With these definitions and assumptions, we show requirements for good generation in AE-models.

#### 3.2. Conditions for Good Generation

An AE-based generative model would attempt to learn continuous functions  $E_\kappa \triangleq g : \mathbb{R}^d \rightarrow \mathbb{R}^m$  and  $D_\psi \triangleq g' : \mathbb{R}^m \rightarrow \mathbb{R}^d$  via some deep enough structure of neural networks. We refer to the dimension to which the Encoder maps the data as  $m$ , the *assumed latent dimension*. As discussed earlier, for good quality data generation the following conditions are to be satisfied:

R1  $\|f(\tilde{z}) - g'(g(f(\tilde{z})))\| = 0 \forall \tilde{z} \in \mathbb{R}^n$ , where  $\|\cdot\|$  denotes some norm. This condition states that the reconstruction error between the real and generated data should be minimal.

R2 The Kullback-Leibler divergence,  $D_{KL}(\Pi||\Psi)$  between the chosen prior  $\Pi$ , and  $\Psi$  on  $\mathcal{Z}$  is minimal<sup>1</sup>.

With this, we state and prove the conditions required to ensure R1 and R2 are met.

**Theorem 1.** *With the assumption of data generating process mentioned in Sec.3.1, requirements R1 and R2 (Sec.3.2), can be satisfied iff true latent dimension  $n$  is equal to assumed latent dimension  $m$ .*

**Proof:** We prove by contradicting either R1 or R2, in assuming both the cases of  $m < n$  or  $m > n$ .

*Case A :  $m < n$  :* Since  $f$  is injective and differentiable everywhere, it must have a continuous left inverse (call it  $f^{-1}$ ). Also, the R1 forces  $g'$  to be the left inverse of  $g$  on the range of  $f$ . Since  $g$  and  $g'$  are both neural networks, the composite  $g \circ f$  has a continuous left inverse  $f^{-1} \circ g'$  which is impossible due to the following lemma:

**Lemma 1:** A continuous function  $\phi : \mathbb{R}^\alpha \rightarrow \mathbb{R}^\beta$  cannot have a continuous left inverse if  $\alpha > \beta$ .

**Proof:** It follows trivially from the fact that such a function would define a homeomorphism from  $\mathbb{R}^\alpha$  to a subset of  $\mathbb{R}^\beta$ , whereas it is well known that these two spaces are not homeomorphic.  $\square$

This implies that R1 and Lemma 1 contradict each other in

<sup>1</sup>Subsequent results can be extended to any other divergence metric.

the case  $m < n$  and thus to obtain a good reconstruction,  $m$  should at-least be equal to  $n$ .

*Case B :  $m > n$  :* For the sake of simplicity, let us assume that  $\tilde{\mathcal{Z}}$  is a unit cube in  $\mathbb{R}^{n^2}$ . We show that in this case, R2 will be contradicted if  $m > n$  in Lemma 2 and 3. The idea is to first show that the range of  $g \circ f$  will have Lebesgue measure 0 (Lemma 2) and this leads to arbitrarily large  $D_{KL}$  (Lemma 3).

**Lemma 2:** Let  $\Omega : [0, 1]^n \rightarrow \mathbb{R}^m$  be an  $L$ -lipschitz function. Then its range  $R \in \mathbb{R}^m$  has Lebesgue measure 0 in  $m$  dimensions in  $m > n$ .

**Proof:** For some  $\epsilon \in \mathbb{N}$ , consider the set of points:

$$S = \left\{ \left( \frac{a_0 + 0.5}{\epsilon}, \dots, \frac{a_{n-1} + 0.5}{\epsilon} \right) \mid a_i \in \{0, \dots, \epsilon - 1\} \right\}.$$

Construct closed balls around then having radius  $\frac{\sqrt{n}}{2\epsilon}$ . It is easy to see that every point in the domain of  $\Omega$  is contained in at least one of these balls. This is because, for any given point, the nearest point in  $S$  can be at-most  $\frac{1}{2\epsilon}$  units away along each dimension. Also, since  $\Omega$  is  $L$ -lipschitz, we can conclude that the image set of a closed ball having radius  $r$  and centre  $\mathbf{u} \in [0, 1]^n$  would be a subset of the closed ball having centre  $\Omega(\mathbf{u})$  and radius  $L \times r$ .

The range of  $\Omega$  is then a subset of the union of the image sets off all the closed balls defines around  $S$ . The volume of this set is upper bounded by the sum of the volumes of the individual image balls, each having volume  $\frac{c}{\epsilon^m}$  where  $c$  is a constant having value  $\frac{(L)^m (n\pi)^{\frac{m}{2}}}{\Gamma(\frac{m}{2} + 1)}$ . Therefore,

$$\text{vol}(R) \leq |S| \times \frac{c}{\epsilon^m} = \frac{c}{\epsilon^{m-n}}. \quad (1)$$

The final quantity of Eq. 1 can be made arbitrarily small by choosing  $\epsilon$  appropriately. Since the Lebesgue measure of a closed ball is same as its volume, the range of  $\Omega$ ,  $R$  has measure 0 in  $\mathbb{R}^m$   $\square$

Since  $f$ ,  $g$  are Lipschitz,  $g \circ f$  must have a range with Lebesgue measure 0 as a consequence of Lemma 2. Now we show that as a consequence of the range of  $g \circ f$  (call it  $\mathcal{R}$ ) of having measure 0, the KL divergence between  $\Pi$  and  $\Psi$  goes to infinity.

**Lemma 3:** If  $\Pi$  and  $\Psi$  are two distributions as defined in Sec.3.1 such that the support of the latter has a 0 Lebesgue measure, then  $D_{KL}(\Pi \parallel \Psi)$  grows to be arbitrarily large.

<sup>2</sup>One can easily obtain another function  $\nu : [0, 1]^n \rightarrow \tilde{\mathcal{Z}}$  that scales and translates the unit cube appropriately. Note that for such a  $\nu$  to exist, we need  $\tilde{\mathcal{Z}}$  to be bounded, which may not be the case for certain distributions like the Gaussian distributions. Such distributions, however, can be approximated successively in the limiting sense by truncating at some large value [31]

**Proof:** To begin with,  $\Psi$  can be equivalently expressed as:

$$\Psi(\mathbf{z}) = \begin{cases} \tilde{\Psi}(\tilde{\mathbf{z}}) & \text{if } \exists \tilde{\mathbf{z}}^3 \in \tilde{\mathcal{Z}} \text{ s.t. } g(f(\tilde{\mathbf{z}})) = \mathbf{z}, \\ 0 & \text{otherwise} \end{cases} \quad (2)$$

Define  $\mathbb{I}_{\mathcal{R}}$  as the indicator function of  $\mathcal{R}$ , i.e.

$$\mathbb{I}_{\mathcal{R}}(\mathbf{z}) = \begin{cases} 1 & \text{if } \exists \tilde{\mathbf{z}} \in \tilde{\mathcal{Z}} \text{ s.t. } g(f(\tilde{\mathbf{z}})) = \mathbf{z}, \\ 0 & \text{otherwise} \end{cases} \quad (3)$$

Since  $\mathcal{R}$  has measure 0 (Lemma 2), we have

$$\int_{\mathbb{R}^m} \mathbb{I}_{\mathcal{R}}(\mathbf{z}) d\mathbf{z} = 0 \quad (4)$$

Further, since  $\mathbb{I}_{\mathcal{R}}$  is identically 1 in the support of  $\Psi$ , we have

$$\Psi(\mathbf{z}) = \Psi(\mathbf{z}) \mathbb{I}_{\mathcal{R}}(\mathbf{z}) \quad (5)$$

Now consider the cross-entropy between  $\Pi$  and  $\Psi$  given by:

$$\begin{aligned} \mathcal{H}(\Pi, \Psi) &= \int_{\mathcal{Z}} \Pi(\mathbf{z}) (-\log(\Psi(\mathbf{z}))) d\mathbf{z} \\ &\geq \int_{\mathcal{Z}-\mathcal{R}} \Pi(\mathbf{z}) (-\log(\Psi(\mathbf{z}) \mathbb{I}_{\mathcal{R}}(\mathbf{z}))) d\mathbf{z} \quad (6) \\ &\geq \varrho \int_{\mathcal{Z}-\mathcal{R}} \Pi(\mathbf{z}) d\mathbf{z} \end{aligned}$$

for any arbitrarily large positive real  $\varrho$ . This holds because  $\mathbb{I}_{\mathcal{R}}$  is identically 0 over the domain of integration. Further,

$$\begin{aligned} \int_{\mathcal{Z}-\mathcal{R}} \Pi(\mathbf{z}) &\geq \int_{\mathcal{Z}} \Pi(\mathbf{z}) - \int_{\mathcal{R}} \Pi(\mathbf{z}) \\ &= 1 - \int_{\mathbb{R}^m} \Pi(\mathbf{z}) \mathbb{I}_{\mathcal{R}}(\mathbf{z}) d\mathbf{z} \quad (7) \\ &\geq 1 - \max_{\mathbb{R}^m}(\Pi(\mathbf{z})) \int_{\mathbb{R}^m} \mathbb{I}_{\mathcal{R}}(\mathbf{z}) d\mathbf{z} \\ &= 1 \end{aligned}$$

Combining 6 and 7, the required cross-entropy is lower bounded by an arbitrarily large quantity  $\varrho$ . Since cross entropy and KL-divergence differ only by the entropy of  $\Pi$  which is finite, the KL-divergence is arbitrarily large.  $\square$  Thus Lemma 3 contradicts R2 required for good generation in the case  $m > n$ . Therefore, neither  $m > n$  nor  $m < n$  can be true if good generation has to be ensured. Thus, one must have  $m = n$  (concludes Theorem 1).  $\square$

One can ensure good generation by a trivial solution in the form of  $g' = f$  with an appropriate  $g$  and making  $m = n$ . However, since neither  $n$  nor  $f$  is known, one needs a practical method to ensure  $m$  to approach  $n$  which is described in the next section.

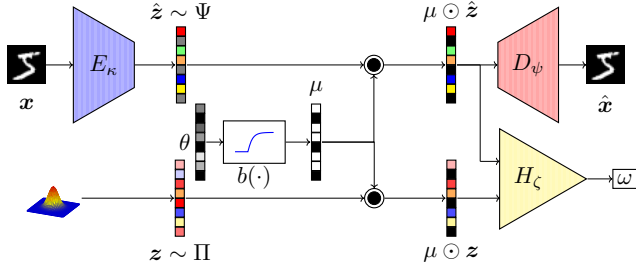


Figure 2. Block Diagram of Latent Masked Generative Auto Encoder. LMGAE consists of three pipelines: reconstruction pipeline consisting of  $E_{\kappa}$ ,  $\mu$ , and  $D_{\psi}$ ; Masking pipeline consisting of  $\theta$ ,  $b$  and  $\mu$ ; and Distribution-Matching pipeline consisting of  $E_{\kappa}$ ,  $\mu$ , and  $H_{\zeta}$ .

#### 4. Latent Masked Generative AE (LMGAE)

In this section, we take the ideas presented in Section 3, and build an architecture such that the true latent dimension of the underlying data distribution could potentially be discovered in an AE set-up, resulting in better generation quality. Our key intuition lies in the following insight: if we start with a large enough estimated latent space dimension, and then give our model an ability to train a mask, which could suppress the set of spurious dimensions, then the model would automatically discover the right number of latent dimensions (which are not masked). This is via minimizing the combination of (1) Re-construction loss (2) A divergence loss, i.e.,  $R1$  and  $R2$ , in Section 3, respectively. We next describe the details of our architecture followed by the details of the corresponding loss function which we minimize over this architecture. Figure 2 presents our model architecture. There are three components to it as follows:

1. **Re-construction Pipeline:** This is the standard pipeline in any given AE based model, which tries to minimize the reconstruction loss (R1). An input sample  $x$  is passed through the encoder  $E_{\kappa}$  results in  $\hat{z}$ , the corresponding representation in the latent space. The new addition here is the Hadamard product with the mask  $\mu$  (explained next), resulting in the masked latent space representation  $\mu \odot \hat{z}$ . The masked representation is then fed to the decoder  $D_{\psi}$  to obtain the re-constructed output  $\hat{x}$ . The goal here is to minimize the norm of the difference between  $x$  and  $\hat{x}$ .
2. **Masking Pipeline:** Introduction of a mask is one of the novel contributions of our work, and this is the second part of our architecture presented in the middle of the Figure 2. Our mask is represented as  $\mu$  and is a binary vector of size  $m$  (model capacity). Ideally, the mask would be a binary vector, but in order to make it learnable, we relax it to be continuous valued, while

<sup>3</sup>Note that this  $\tilde{z}$  is guaranteed to be unique because  $f$  is injective by A1 and  $g$  is injective in the range of  $f$  from R1.

imposing certain regularizers so that it does not deviate too much from 0 or 1 during learning. Specifically, we parameterize  $\mu$  using a vector  $\theta \in \mathcal{R}$  such that  $\mu = b(\theta)$  where  $b(\theta) = \max(0, 1 - e^{-\theta})$ . Intuitively, this parameterization forces  $\mu$  to be close to 0 or 1.

3. **Distribution-Matching Pipeline:** This is the third part of our architecture presented at the bottom of Figure 2. Objective of this pipeline is to minimize the distribution loss between a prior distribution,  $\Pi$ , and the distribution  $\Psi$  imposed on the latent space by the encoder.  $z$  is a random vector sampled from the prior distribution, whose Hadamard product is taken with the mask  $\mu$  (similar to in the case of encoder), resulting in a masked vector  $\mu \odot z$ . This masked vector is then passed through the network  $H_{\zeta}$ , where the goal is to separate out the samples coming from prior distribution ( $z$ ) from those coming from the encoded space ( $\hat{z}$ ) using some divergence metric. We use the principles detailed in [3] using the Wasserstein's distance to measure the distributional divergence. Note that  $H_{zeta}$  has two inputs namely, samples of  $\Pi(z)$  and output of  $E_{kappa}$ .

Intuitively, masking of the latent space vector ( $\hat{z}$ ) and the sampled vector ( $z$ ) allows us to work only with a subset of dimensions in the latent space. This means that though  $m$  may be greater than  $n$ , we can use the idea of masking, to effectively work in an  $\mathcal{R}^n$  dimensional space, satisfying the conditions of our theory for minimizing the combined loss over  $R1$  and  $R2$  (Section 3). Next, corresponding to each of the components above, we present a loss function where  $s$  represents the batch size.

1. **Auto-Encoder Loss:** This is the standard loss to capture the quality of re-construction as used earlier in the AE literature. In addition, we have a term corresponding to minimization of the variance over the masked dimensions in the encoded output in a batch. The intuition is that encoder should not inject information into the dimensions which are going to be masked anyway. The loss is specified as:

$$L_{ae} = \frac{\alpha_1}{s} \sum_{i=1}^s \|\mathbf{x}^{(i)} - D_{\psi}(\mu \odot E_{\kappa}(\mathbf{x}^{(i)}))\| + \alpha_2(\delta^T \text{Diag}(A)) \quad (8)$$

$A$  represents the co-variance matrix for the encoding matrix  $E_{\kappa}(X)$ ,  $X$  being the data matrix for the current batch.  $\delta$  is the vector obtained by applying the function  $a(u) = e^{-\gamma \times u}$  point-wise to  $\mu$ .  $\alpha_1$ ,  $\alpha_2$  and  $\gamma$  are hyperparameters.

2. **Generator Loss:** This is the loss capturing the quality of generation in terms of how far is it from the prior

distribution. This loss measures the ability of the encoder to generate the samples such that they are coming from  $\Pi(\mathbf{z})$  which is ensured using the generator loss mentioned in [3]:

$$L_{gen} = -\frac{1}{s} \sum_{i=1}^s H_{\zeta}(\mu \odot E_{\kappa}(\mathbf{x}^{(i)})) \quad (9)$$

3. **Distribution-Matching Loss:** This is the loss incurred by the Distribution-matching network,  $H_{\zeta}$  in matching the distributions. We use Wasserstein’s distance [3] to measure the distributional closeness with the following loss:

$$\begin{aligned} L_{dm} = & -\frac{1}{s} \sum_{i=1}^s H_{\zeta}(\mu \odot \mathbf{z}^{(i)}) + \frac{1}{s} \sum_{i=1}^s H_{\zeta}(\mu \odot \hat{\mathbf{z}}^{(i)}) \\ & + \frac{\beta_2}{s} \sum_{i=1}^s (\|\nabla_{\mathbf{z}_{avg}^{(i)}} H_{\zeta}(\mu \odot \mathbf{z}_{avg}^{(i)})\| - 1)^2 \end{aligned} \quad (10)$$

Recall that  $\hat{\mathbf{z}}^{(i)} = E_{\kappa}(\mathbf{x}^{(i)})$ . Further, we have used  $\mathbf{z}_{avg}^{(i)} = \beta_1 \mathbf{z}^{(i)} + (1 - \beta_1) \hat{\mathbf{z}}^{(i)}$ .  $\beta_1, \beta_2$  are hyper parameters, with  $\beta_1 \sim \mathcal{U}[0, 1]$ , and  $\beta_2$  set as in [13].

4. **Masking Loss:** This is the loss capturing the quality of the current mask. The loss is a function of three terms (1) Auto-encoder loss (2) distribution matching loss (3) a regularizer to ensure that  $\mu$  parameters stay close to 0 or 1. This can be specified as:

$$\begin{aligned} L_{mask} = & \frac{\lambda_1}{s} \sum_{i=1}^s \|\mathbf{x}^{(i)} - D_{\psi}(\mu \odot E_{\kappa}(\mathbf{x}^{(i)}))\| \\ & + \lambda_2(1 + \omega)^2 + \lambda_3 \sum_{j=1}^m |\mu_j(\mu_j - 1)| \end{aligned} \quad (11)$$

where  $\omega = \frac{1}{s} \sum_i H_{\zeta}(\mu \odot \mathbf{z}^{(i)}) - \frac{1}{s} \sum_i H_{\zeta}(\mu \odot E_{\kappa}(\mathbf{x}^{(i)}))$  is the Wasserstein’s distance. Here  $\lambda_1$  and  $\lambda_2$  and  $\lambda_3$  are hyper-parameters.

**Training:** During training, we optimize each of the four losses specified above in turn. Specifically, in each learning loop, we optimize the  $L_{ae}$ ,  $L_{dm}$ ,  $L_{gen}$  and  $L_{mask}$ , in that order using a learning schedule. We use RMSProp for our optimization.

## 5. Experiments and Results

We divide our experiments into two parts: (a) Synthetic, and (b) Real. In synthetic experiments, we control the data generation process, with a known number of true latent dimensions. Hence, we can compare the performance of our

proposed model for different number of true latent dimensions, and examine whether our method can discover the true number of latent dimensions. This also helps us validate some of the theoretical claims made in Section 3. On the other hand, the goal in real experiments is to examine whether our masking based approach can result in generation quality which can beat the state-of-the-art AE-based models, given sufficient model capacity. We would also like to understand the behaviour of the number of dimensions which are masked in this case (though the precise number of latent data dimensions may not be known).

### 5.1. Synthetic Experiments

In the following description, we will use  $n$  to denote the true data latent dimension, and  $m$  to denote the estimated latent dimension (i.e, the one used by LMGAE) in line with the notation used earlier in the paper. We will often refer to  $m$  as the model capacity. We are interested in the answering the following question: assuming that data is generated according to the generation process described in Section 3, (a) Given sufficient model capacity (i.e,  $m \geq n$  and sufficiently powerful  $E_{\kappa}$ ,  $D_{\psi}$  and  $H_{\zeta}$ ), can LMGAE discover the true number of latent dimensions? (b) What is the quality of the data generated by LMGAE for varying values of  $m$ ?

In the ideal scenario, we would expect that whenever  $m \geq n$ , the number of dimensions masked by LMGAE are exactly those not required, i.e, the difference between  $m$  and  $n$ . Further, we would expect that the performance of LMGAE is independent of the value of  $m$ , whenever  $m \geq n$ . The performance is expected to deteriorate for values of  $m < n$ . In order to do a comparison, for each value of  $m$  that we experimented with, we also trained an equivalent WAE model with exactly the same architecture as ours but with no masking. We would expect the performance of the WAE model to deteriorate in cases whenever  $m < n$  or  $m > n$  if our theory were to hold correct.

For the synthetic case, we experiment with the data generated using the following process.

- Sample  $\tilde{\mathbf{z}} \sim \mathcal{N}(\mu_s, \Sigma_s)$ , where the mean  $\mu_s \in \mathbb{R}^n$  was fixed to be zero and  $\Sigma_s \in \mathbb{R}^{n \times n}$  represents the diagonal co-variance matrix (isotropic Gaussian).
- Compute  $\mathbf{x} = f(\tilde{\mathbf{z}})$ , where  $f$  is a non-linear function computed using a two-layer fully connected neural network with  $k$  units in each layer,  $d \gg n$  output units, and using leaky ReLU as the non-linearity. The weights of these networks are randomly fixed and  $k$  was taken as 128.

In our experiments, we set  $n = 8$  and 16, and varied  $m$  in the range of [2, 32] for  $n = 8$  and [2, 78] for  $n = 16$  at intervals of 2 in each case. We use the standard Fréchet Inception Distance (FID) [14] score between generated and real

images to validate the quality of the generated data. Figure 3 (a) and (b) presents our results on synthetic data. On X-axis, we plot  $m$ . Y-axis (left) plots the FID score comparing LMGAE and WAE for different values of  $m$ . Y-axis (right) plots the number of active dimensions discovered by our algorithm. In both the figures, both the approaches achieve the best FID score when  $m = n$ . But whereas the performance for WAE deteriorates with increasing  $m$ , LMGAE retains the optimal FID score independent of the value of  $m$ . Further, in each case, we get very close to the true number of latent dimensions, even with different values of  $m$  (as long as  $m > 8$  or  $16$ , respectively). This clearly validates our theoretical claims, and also the fact that LMGAE is capable of offering good quality generation in practice.

## 5.2. Real Datasets

In this section, we examine the behavior of LMGAE on real-world datasets. In this case, the true latent data dimensions ( $n$ ) is unknown, but we can still analyze the behavior as the estimated latent number of dimension ( $m$ ) is varied. We work on four image datasets used extensively in the literature: (a) MNIST [25] (b) Fashion MNIST [38] (c) CIFAR-10 [22] (d) CelebA [26]. We use the same test/train splits as used in the earlier literature.

In our first set of experiments, we perform an analysis similar to the one done in the case of synthetic data, for the MNIST. Specifically, we varied the estimated latent dimension (model capacity  $m$ ) for MNIST from 10 to 110, and analyzed the FID score, as well as number of true dimensions discovered by the model. For comparison, we also did the same experiment using the WAE model. Figure 3 (c) shows the results. As in the case of synthetic data, we observe a U-shape behavior for the WAE model, with the lowest value achieved at  $m = 13$ . This validates our thesis that the best performance is achieved at a specific value of latent dimension, which is supposedly around 13 in this case<sup>4</sup> Further, looking at LMGAE curve, we notice that the performance (FID score) more or less stabilizes (it varies between 10 and 17) for values of  $m \geq 10$ . In addition, the true latent dimension discovered also stabilizes around 10 – 13 irrespective of  $m$ , without compromising much on the generation quality. Note that the same network architecture was used at all points of Figure 3. These observations are in line with the expected behavior of our model, and the fact that our model can indeed mask the spurious set of dimensions to achieve good generation quality.

Figure 5 shows the behaviour of mask for model capacity  $m = 32, 64$  and  $110$  on MNIST dataset. Interestingly, in each case, we are able to discover almost the same number of unmasked dimensions, independent of the starting

<sup>4</sup>True latent dimension is not known in this case. In fact, it is only an assumption that the dataset is generated using the data generation process described in section 3.1.

point. It is also observed that the Wasserstein distance is minimized at the point where the masks reaches the optimal point.

Finally to measure the generation quality, we present the FID scores of our method along with several state-of-the-art AE-based models mentioned in section 2 in Table 1. Clearly, our approach achieves the best FID score on all the datasets compared to the state-of-the-art AE based generative models. Performance of LMGAE is also comparable to that of GANs [27], despite using a simple norm based reconstruction loss and an isotropic uni-modal Gaussian prior. Figure 4 shows some non-cherry-picked samples generated by our algorithm for each of the datasets.

The better FID scores of LMGAE can be attributed to better distribution matching in the latent space between  $\Psi(z)$  and  $\Pi(z)$ . But quantitatively comparing the matching between the two distributions is not easy as LMGAE might mask out some of the latent dimensions resulting in a mismatch between the dimensionality of latent space in different models, thus rendering the usual metrics undefined. We therefore calculate the average off-diagonal co-variance  $Cov$  of the encoded latent vectors and report it in Table 2. Since  $\Pi(z)$  is assumed to be an isotropic Gaussian, ideally  $Cov$  should be zero and any deviation from zero indicates a mismatch. For LMGAE we only use the unmasked latent dimensions for the  $cov$  calculation, this is to ensure that  $cov$  is not underestimated by considering the unused dimension. It is observed that for the same model capacity LMGAE has considerably less  $Cov$  than the corresponding WAE indicating better distribution matching.

	MNIST	Fashion	CIFAR-10	CelebA
VAE (cross-entr.) [20]	16.6	43.6	106.0	53.3
VAE (fixed variance) [20]	52.0	84.6	160.5	55.9
VAE (learned variance) [20]	54.5	60.0	76.7	60.5
VAE + Flow [19]	54.8	62.1	81.2	65.7
WAE-MMD [35]	115.0	101.7	80.9	62.9
WAE-GAN [35]	12.4	31.5	93.1	66.5
2-Stage VAE [10]	12.6	29.3	72.9	44.4
LMGAE	<b>10.5</b>	<b>25.4</b>	<b>71.9</b>	<b>40.5</b>

Table 1. FID scores for generated images from different AE-based generative models (Lower the better).

Dataset	Model Capacity	WAE		LMGAE	
		$m_A$	$Cov$	$m_A$	$Cov$
Synthetic <sub>8</sub>	16	16	0.040	9	<b>0.030</b>
Synthetic <sub>16</sub>	32	32	0.031	16	<b>0.013</b>
MNIST	64	64	0.027	13	<b>0.020</b>
FMNIST	128	128	0.025	40	<b>0.019</b>
CIFAR-10	256	256	0.017	120	<b>0.013</b>
CelebA	256	256	0.046	77	<b>0.039</b>

Table 2. Average off-diagonal covariance  $Cov$  for both WAE and LMGAE.  $m_A$  represents the number of unmasked latent dimensions in the trained model. It is seen that LMGAE has lower  $Cov$  values indicating lesser deviation of  $\Psi(z)$  from  $\Pi(z)$  as compared to a WAE.

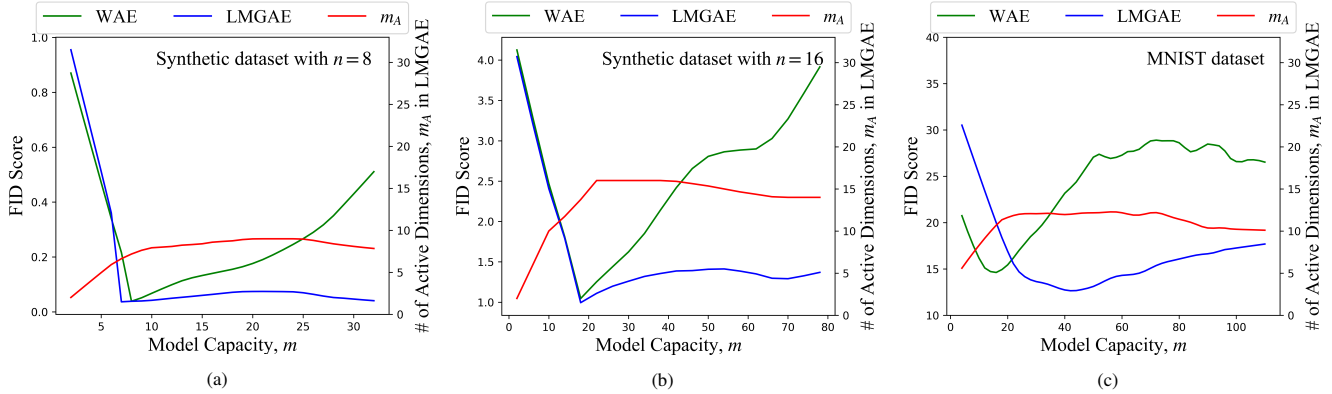


Figure 3. (a) and (b) shows FID score for WAE and LMGAE and active dimension in a trained LMGAE model with varying model capacity,  $m$  for synthetic dataset of true latent dimensions,  $n = 8$  and  $n = 16$ ,  $m_A$  represents the number of unmasked latent dimensions in the trained model and (c) shows the same plots for MNIST dataset.

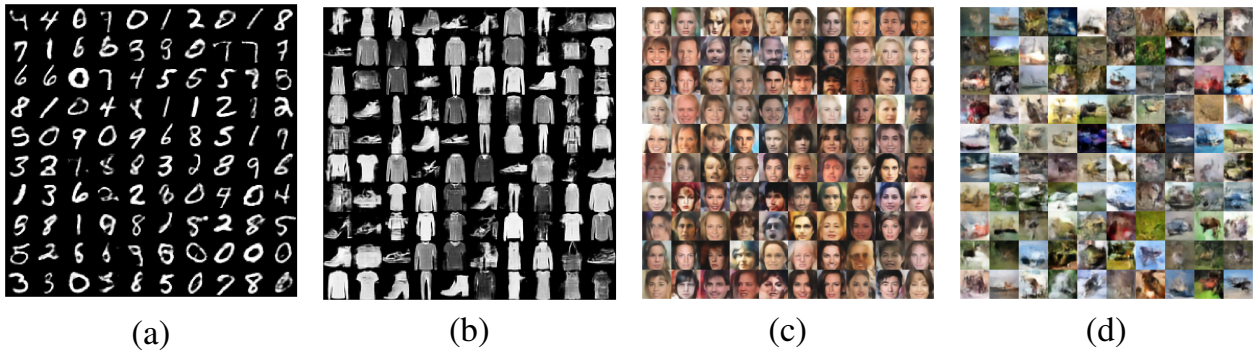


Figure 4. Randomly generated (no cherry picking) images of (a) MNIST, (b) Fashion MNIST, (c) CelebA, and (d) CIFAR-10 datasets.

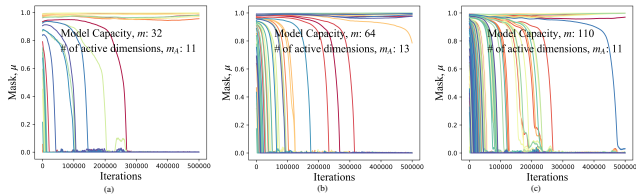


Figure 5. Behaviour of mask in LMGAE models with different  $m$  for the MNIST dataset. Model capacity,  $m$ , in figure (a), (b), and (c) are 32, 64, and 110, respectively. The active dimensions after training are  $m_A$  are 11, 13, and 11 respectively.

These results clearly demonstrate that not only LMGAE can achieve the best FID scores on a number of benchmark datasets, it also gives us a practical handle on potentially discovering the true set of latent dimensions in real as well as artificial data. To the best of our knowledge, this is the first study analyzing (and discovering) the effect of latent dimensions on the generation quality.

## 6. Discussion and Conclusions

Despite demonstrating its pragmatic success, we critically analyze the possible deviations of the practical cases from the presented analysis. More often than not, the naturally occurring data contains some noise superimposed onto

the actual image. Thus, theoretically one can argue that this noise can be utilized to minimize the divergence between the distributions. Practically, however, this noise has very low amplitude, so it can only work for a few extra dimensions, giving a slight overestimate of  $n$ . Further, in practice, not all latent dimensions contribute equally to the data generation. Since the objective of our model is to ignore noise dimensions, it can at times end up throwing away meaningful data dimensions which do not contribute significantly. This can lead to a slight underestimate of  $n$  (which is observed at times during experimentation). Finally, neural networks, however deep, can represent only a certain level of complexity in a function. This is both good and bad for our purposes. It is good because while we have shown that certain losses cannot be made zero for  $m \neq n$ , universal approximators can bring them arbitrarily close to zero, which is practically the same thing. Due to their limitation, however, we end up getting a U-curve. It is bad because even at the  $m \geq n$ , the encoder and decoder networks might be unable to learn the appropriate functions, and at  $m \leq n$  the  $H_C$  fails to make distributions apart. This implies that instead of discovering the exact same number of dimensions every time, we might get a range of values near the true latent dimension. Also, the severity of this problem is likely

to increase with the complexity of the dataset (again corroborated by the experiments).

To conclude, in this work, we have taken a step towards constructing an optimal latent space for improving the generation quality of Auto-Encoder based neural generative model. We have argued that, under the assumption two-step generative process to natural data, the optimal latent space for the AE-model is one where its dimensionality matches with that of the latent space of the generative process. Further, we have proposed a practical method to arrive at this optimal dimensionality from an arbitrary point.

## References

- [1] Guillaume Alain and Yoshua Bengio. What regularized auto-encoders learn from the data-generating distribution. *The Journal of Machine Learning Research*, 15(1):3563–3593, 2014. [2](#)
- [2] Martin Arjovsky and Léon Bottou. Towards principled methods for training generative adversarial networks. *arXiv*. 2017. [1](#)
- [3] Martin Arjovsky, Soumith Chintala, and Léon Bottou. Wasserstein generative adversarial networks. In *International conference on machine learning*, pages 214–223, 2017. [5](#), [6](#)
- [4] Sanjeev Arora, Rong Ge, Yingyu Liang, Tengyu Ma, and Yi Zhang. Generalization and equilibrium in generative adversarial nets (gans). In *Proceedings of the 34th International Conference on Machine Learning-Volume 70*, pages 224–232. JMLR. org, 2017. [1](#)
- [5] Matthias Bauer and Andriy Mnih. Resampled priors for variational autoencoders. *arXiv preprint arXiv:1810.11428*, 2018. [1](#), [2](#)
- [6] Andrew Brock, Jeff Donahue, and Karen Simonyan. Large scale gan training for high fidelity natural image synthesis. *arXiv preprint arXiv:1809.11096*, 2018. [1](#)
- [7] Christopher P Burgess, Irina Higgins, Arka Pal, Loic Matthey, Nick Watters, Guillaume Desjardins, and Alexander Lerchner. Understanding disentangling in beta -vae. *arXiv preprint arXiv:1804.03599*, 2018. [2](#)
- [8] Lawrence Cayton. Algorithms for manifold learning. *Univ. of California at San Diego Tech. Rep*, 12(1-17):1, 2005. [1](#)
- [9] Tian Qi Chen, Xuechen Li, Roger B Grosse, and David K Duvenaud. Isolating sources of disentanglement in variational autoencoders. In *Advances in Neural Information Processing Systems*, pages 2610–2620, 2018. [2](#)
- [10] Bin Dai and David Wipf. Diagnosing and enhancing vae models. *arXiv preprint arXiv:1903.05789*, 2019. [1](#), [2](#), [3](#), [7](#)
- [11] Ian Goodfellow, Jean Pouget-Abadie, Mehdi Mirza, Bing Xu, David Warde-Farley, Sherjil Ozair, Aaron Courville, and Yoshua Bengio. Generative adversarial nets. In Z. Ghahramani, M. Welling, C. Cortes, N. D. Lawrence, and K. Q. Weinberger, editors, *Advances in Neural Information Processing Systems 27*, pages 2672–2680. Curran Associates, Inc., 2014. [1](#)
- [12] Aditya Grover, Manik Dhar, and Stefano Ermon. Flow-gan: Bridging implicit and prescribed learning in generative models. *arXiv preprint arXiv:1705.08868*, 2017. [1](#)
- [13] Ishaan Gulrajani, Faruk Ahmed, Martin Arjovsky, Vincent Dumoulin, and Aaron Courville. Improved training of wasserstein gans, 2017. [6](#)
- [14] Martin Heusel, Hubert Ramsauer, Thomas Unterthiner, Bernhard Nessler, and Sepp Hochreiter. Gans trained by a two time-scale update rule converge to a local nash equilibrium. In I. Guyon, U. V. Luxburg, S. Bengio, H. Wallach, R. Fergus, S. Vishwanathan, and R. Garnett, editors, *Advances in Neural Information Processing Systems 30*, pages 6626–6637. Curran Associates, Inc., 2017. [6](#)
- [15] Irina Higgins, Loic Matthey, Arka Pal, Christopher Burgess, Xavier Glorot, Matthew Botvinick, Shakir Mohamed, and Alexander Lerchner. beta-vae: Learning basic visual concepts with a constrained variational framework. *ICLR*, 2(5):6, 2017. [2](#)
- [16] Matthew D Hoffman and Matthew J Johnson. Elbo surgery: yet another way to carve up the variational evidence lower bound. In *Workshop in Advances in Approximate Bayesian Inference, NIPS*, volume 1, 2016. [2](#)
- [17] Yedid Hoshen, Ke Li, and Jitendra Malik. Non-adversarial image synthesis with generative latent nearest neighbors. In *Proceedings of the IEEE Conference on Computer Vision and Pattern Recognition*, pages 5811–5819, 2019. [1](#), [2](#)
- [18] Hyunjik Kim and Andriy Mnih. Disentangling by factorising. *arXiv preprint arXiv:1802.05983*, 2018. [2](#)
- [19] Durk P Kingma, Tim Salimans, Rafal Jozefowicz, Xi Chen, Ilya Sutskever, and Max Welling. Improved variational inference with inverse autoregressive flow. In *Advances in neural information processing systems*, pages 4743–4751, 2016. [1](#), [2](#), [7](#)
- [20] Diederik P Kingma and Max Welling. Auto-encoding variational bayes, 2013. [1](#), [2](#), [7](#)
- [21] Alexej Klushyn, Nutan Chen, Richard Kurle, Botond Cseke, and Patrick van der Smagt. Learning hierarchical priors in vaes. *arXiv preprint arXiv:1905.04982*, 2019. [1](#), [2](#)
- [22] Alex Krizhevsky. Learning multiple layers of features from tiny images. Technical report, 2009. [7](#)
- [23] Vinay Kyatham, Deepak Mishra, Tarun Kumar Yadav, Dheeraj Mundhra, et al. Variational inference with latent space quantization for adversarial resilience. *arXiv preprint arXiv:1903.09940*, 2019. [3](#)
- [24] Martin HC Law and Anil K Jain. Incremental nonlinear dimensionality reduction by manifold learning. *IEEE transactions on pattern analysis and machine intelligence*, 28(3):377–391, 2006. [1](#)
- [25] Y. Lecun. The mnist database of handwritten digits. <http://yann.lecun.com/exdb/mnist/>, 2010. [2](#), [7](#)
- [26] Ziwei Liu, Ping Luo, Xiaogang Wang, and Xiaoou Tang. Deep learning face attributes in the wild. In *Proceedings of International Conference on Computer Vision (ICCV)*, December 2015. [7](#)
- [27] Mario Lucic, Karol Kurach, Marcin Michalski, Sylvain Gelly, and Olivier Bousquet. Are gans created equal? a large-scale study. In *Advances in neural information processing systems*, pages 700–709, 2018. [7](#)

- [28] Alireza Makhzani, Jonathon Shlens, Navdeep Jaitly, and Ian Goodfellow. Adversarial autoencoders. In *International Conference on Learning Representations*, 2016. [1](#), [2](#)
- [29] Hariharan Narayanan and Sanjoy Mitter. Sample complexity of testing the manifold hypothesis. In *Advances in Neural Information Processing Systems*, pages 1786–1794, 2010. [1](#)
- [30] Danilo Jimenez Rezende and Shakir Mohamed. Variational inference with normalizing flows. *arXiv preprint arXiv:1505.05770*, 2015. [2](#)
- [31] Walter Rudin et al. *Principles of mathematical analysis*, volume 3. McGraw-hill New York, 1964. [4](#)
- [32] Tim Salimans, Ian Goodfellow, Wojciech Zaremba, Vicki Cheung, Alec Radford, and Xi Chen. Improved techniques for training gans. In *Advances in neural information processing systems*, pages 2234–2242, 2016. [1](#)
- [33] Akash Srivastava, Lazar Valkov, Chris Russell, Michael U Gutmann, and Charles Sutton. Veegan: Reducing mode collapse in gans using implicit variational learning. In *Advances in Neural Information Processing Systems*, pages 3308–3318, 2017. [1](#)
- [34] Lucas Theis, Aäron van den Oord, and Matthias Bethge. A note on the evaluation of generative models. *arXiv preprint arXiv:1511.01844*, 2015. [1](#)
- [35] Ilya Tolstikhin, Olivier Bousquet, Sylvain Gelly, and Bernhard Scholkopf. Wasserstein auto-encoders. 2018. [1](#), [2](#), [7](#)
- [36] Jakub M Tomczak and Max Welling. Vae with a vampprior. *arXiv preprint arXiv:1705.07120*, 2017. [1](#), [2](#)
- [37] Aaron van den Oord, Oriol Vinyals, et al. Neural discrete representation learning. In *Advances in Neural Information Processing Systems*, pages 6306–6315, 2017. [1](#), [2](#), [3](#)
- [38] Han Xiao, Kashif Rasul, and Roland Vollgraf. Fashion-mnist: a novel image dataset for benchmarking machine learning algorithms, 2017. [7](#)
- [39] Shengjia Zhao, Jiaming Song, and Stefano Ermon. Infovae: Information maximizing variational autoencoders, 2017. [1](#)